Probing the DNA-Binding Affinity and Specificity of Designed Zinc Finger Proteins

Derek Jantz and Jeremy M. Berg*
Laboratory of Molecular Biology, National Institute of Diabetes and Digestive and Kidney Diseases, Bethesda, Maryland

ABSTRACT Engineered transcription factors and endonucleases based on designed Cys_2His_2 zinc finger domains have proven to be effective tools for the directed regulation and modification of genes. The introduction of this technology into both research and clinical settings necessitates the development of rapid and accurate means of evaluating both the binding affinity and binding specificity of designed zinc finger domains. Using a fluorescence anisotropy-based DNA-binding assay, we examined the DNA-binding properties of two engineered zinc finger proteins that differ by a single amino acid. We demonstrate that the protein with the highest affinity for a particular DNA site need not be the protein that binds that site with the highest degree of specificity. Moreover, by comparing the binding characteristics of the two proteins at varying salt concentrations, we show that the ionic strength makes significant and variable contributions to both affinity and specificity. These results have significant implications for zinc finger design as they highlight the importance of considering affinity, specificity, and environmental requirements in designing a DNA-binding domain for a particular application.

INTRODUCTION

Engineered zinc finger domains are beginning to make significant contributions to functional genomics, synthetic biology, and clinical medicine. Designed site-specific DNA-binding domains based on the zinc finger architecture can be fused to an appropriate transcription effector domain to yield ''custom'' transcription factors suitable for the directed regulation of gene expression (1–5). Recombinant transcription factors containing an array of engineered zinc fingers have been used to regulate a variety of genes in their proper chromosomal contexts in cultured mammalian cells, plants, and animal models (6–8). In addition, engineered endonucleases comprising a designed zinc finger DNA-binding domain fused to the FokI nuclease domain are finding widespread applicability as reagents for targeted genome modification (9–18). Such zinc finger nucleases (ZFNs) have been used to produce user-specified genetic alterations at endogenous loci in a wide range of species, most notably human cells, zebrafish, and higher plants. The canonical zinc finger has a $\beta\beta\alpha$ architecture stabilized by the coordination of a zinc ion by two cysteine and two histidine residues (19–21). Typically, DNA base contacts are made from the major groove by three to four residues within each finger, typically found at positions -1, 2, 3, and 6 relative to the start of the α-helix. Substitutions to these DNA-contacting residues can produce alterations in the DNA-binding specificity, making zinc finger domains well suited to the construction of novel DNA-binding domains by rational design or a variety of selection strategies (1,4,22–37).

It is essential to obtain a thorough characterization of designed proteins in vitro to correlate their DNA-binding properties with any potential biological activity. To this end, methods based on electrophoretic mobility shifts, surface plasmon resonance, and enzyme-linked immunosorbent assay have been used extensively. These existing methods, however, suffer from limitations in speed, the range of conditions under which they can be carried out, and uncertainty with regard to the precise meaning of determined dissociation constants. Many of these difficulties are avoided in fluorescence-anisotropy-based assays in which both the protein and nucleic acid target are free in solution (38–40). In this type of assay, one component of the complex (typically an oligonucleotide) is labeled with an appropriate fluorophore and the anisotropy of this fluorescent species is determined in solution. As protein is added, it binds the labeled oligonucleotide to produce a complex that tumbles more slowly and increases the anisotropy of the fluorophore. Analysis of the anisotropy change as a function of protein concentration produces a binding isotherm from which the dissociation constant for the protein-DNA complex can be determined. An anisotropy-based method was recently used to probe a range of zinc finger-DNA interactions (32).

Anisotropy-based DNA binding assays often employ end-labeled oligonucleotides as the fluorescent species. Initial attempts to develop an assay of this type suitable for Cys_2His_2 zinc finger proteins, however, failed to produce a labeled DNA probe that would undergo a substantial increase in fluorescence anisotropy in response to protein binding. To overcome this problem, we examined a series of probes with the fluorophore placed in a variety of positions along the oligonucleotide, and found that placing the fluorophore on an internal thymidine base significantly increased the anisotropy change that accompanies protein

Submitted August 3, 2009, and accepted for publication November 2, 2009.

*Correspondence: bergj@mail.nih.gov

Derek Jantz's present address is Precision Biosciences, 104 T. W. Alexander Dr., Bldg. 7, Durham, NC 27709.

Editor: Doug Barrick.

0006-3495/10/03/0852/9 $2.00

doi: 10.1016/j.bpj.2009.11.021

binding. We used this assay to examine the binding properties of two zinc finger proteins that differ by a single DNA-contacting residue, and found that they exhibit significant differences in both binding affinity and binding specificity. One zinc finger mutant binds to its preferred DNA site with relatively low affinity, but discriminates well against closely related sequences. The other protein binds to this same DNA site with higher affinity, but does so at the cost of reduced binding specificity. These differences appear to be due to the fact that one protein contains a neutral asparagine residue that is capable of contacting a number of different bases with reasonable affinity, whereas the other contains a negatively charged aspartate that forms a stable contact with cytosine but also interacts electrostatically with the DNA.

MATERIALS AND METHODS

Zinc finger protein expression and purification

The zinc finger protein QNK-QDK-RHR was prepared as described previously (25). The proteins RHR-QDK-QNK and RHR-QDK-QDK were produced using an expressed protein ligation-based strategy, also as previously described (41). Briefly, a region corresponding to the N-terminal two fingers (residues 1–65) was expressed as an intein fusion protein. The C-terminal finger was produced by conventional peptide synthetic methods and ligated to the expressed region. After purification by high-performance liquid chromatography, all proteins were dissolved in 20 mM Tris, pH 7.5, containing 50 mM NaCl and 50 μM $ZnCl_2$, to yield a 10 μM solution of protein (determined based on the absorbance at 274 nm for the protein before zinc addition; $\varepsilon = 4200\ M^{-1}cm^{-1}$). Apparent stoichiometries from binding experiments (discussed below) confirmed that these protein preparations were essentially completely active.

Fluorescence anisotropy-based binding assay

All oligonucleotides were purchased from Operon (Huntsville, AL). A 100 μM solution of fluorescein-dT-labeled oligonucleotide was annealed to a complementary oligonucleotide at 1.5-fold excess by brief incubation at 65° followed by cooling on ice. This double-stranded probe was then added to a 3 mL solution of 20 mM Tris, pH 7.5, containing 100 mM NaCl and 10 μg/mL bovine serum albumin to a final concentration of 10 nM based on the concentration of the labeled strand (experiments to evaluate the effects of ionic strength on binding were conducted at NaCl concentrations of 50 mM, 68.5 mM, 81.5 mM, or 100 mM). This solution was added to a 4.5 mL acrylic cuvette (Fisher) with a micro stir bar, and the fluorescence anisotropy was determined at 25° on a SPEX Fluorolog-2 spectrofluorimeter (Horiba, Edison, NJ) in the L format with the excitation monochrometer set at 490 nM and the emission monochrometer at 515 nM for the fluorescein-labeled probes or 585 nM and 600 nM for the Texas Red-labeled probe (probe 5). Purified protein was added stepwise, and before anisotropy measurements were obtained, the solution was allowed to stand for 5 min (a period of time that has been demonstrated to allow equilibration) at room temperature. The fraction bound (f_B) was determined from the equation

$$f_B = \frac{r - r_{free}}{(r_{bound} - r)Q + (r - r_{free})}$$

where r_{free} is the anisotropy of the free oligonucleotide, r_{bound} is the anisotropy in the presence of saturating amounts of protein, and Q is the ratio of the quantum yields for the bound and free forms. The fraction bound was calculated from the total concentration of protein (P_T), the total concentration of DNA (DNA_T), and the dissociation constant (K_d) from the equation

$$f_B = \frac{[P - DNA]}{DNA_T} = \frac{P_T + DNA_T + K_d - \sqrt{(P_T + DNA_T + K_d)^2 - 4P_T DNA_T}}{2\ DNA_T}$$

where [P-DNA] is the concentration of the protein-DNA complex. The observed binding curves were fit to this equation using Kaleidagraph (Synergy, Reading, PA). All binding experiments were performed in triplicate and standard deviations from the mean in the calculated dissociation constants were calculated. The observed changes in anisotropy were sufficiently large and precise for dissociation constants in the nanomolar range to be determined by fitting the curvature in the binding curves.

Competition experiments to determine specificity

Initial sample preparations were performed as described above. Initially, protein was added to the labeled oligonucleotide solution to achieve ~70% binding of the probe. Unlabeled, double-stranded competitor oligonucleotides in the same buffer were then added in stepwise fashion with a 15-min incubation at room temperature before anisotropy determination. This time was demonstrated to be sufficient to allow stable anisotropy readings implying equilibration. Values for f_B were determined as described with $Q = 0.91$ for probe 8. Anisotropy values were plotted as a function of competitor concentration, and the curves were fit using Mathematica (Wolfram Research, Champaign, IL) to determine the dissociation constants for the protein in complex with competitor oligonucleotides given the previously determined dissociation constant for the labeled probe. The fit curves were based on the exact solution to the cubic equation derived for two ligands competing for a single protein (42).

RESULTS

Comparison of fluorescent DNA probes

To identify a DNA probe suitable for the assay of zinc finger proteins by fluorescence anisotropy, seven fluorescently labeled oligonucleotides were synthesized (Fig. 1 *A*). Each fluorescent oligonucleotide had the same core sequence centered around the nine-basepair binding site (5′-GAG-GCA-GAA-3′) for the previously well-characterized zinc finger protein QNK-QDK-RHR (Fig. 1 *B*). This designed protein, named for the amino acids in the DNA-contacting positions (−1, 3, and 6) in each of its three zinc finger domains, has been characterized crystallographically and extensively investigated with regard to its DNA-binding specificity (43). A schematic structure for this protein aligned with its optimal binding site is shown in Fig. 2 *A*. The labeled oligonucleotides, which differed in overall length, fluorophore location, or fluorophore type, were annealed to a complementary oligonucleotide to generate seven double-stranded DNA probes. A solution of each probe was then added to a fluorescence cuvette and the fluorescence anisotropy of the labeled probe was measured before and after the stepwise addition of purified QNK-QDK-RHR protein (Fig. 1 *C*).

Probes 1–5 showed very little anisotropy change in response to increasing concentrations of zinc finger protein, indicating that conventional end-labeled probes are not useful for the assay of zinc finger-DNA binding. In contrast,

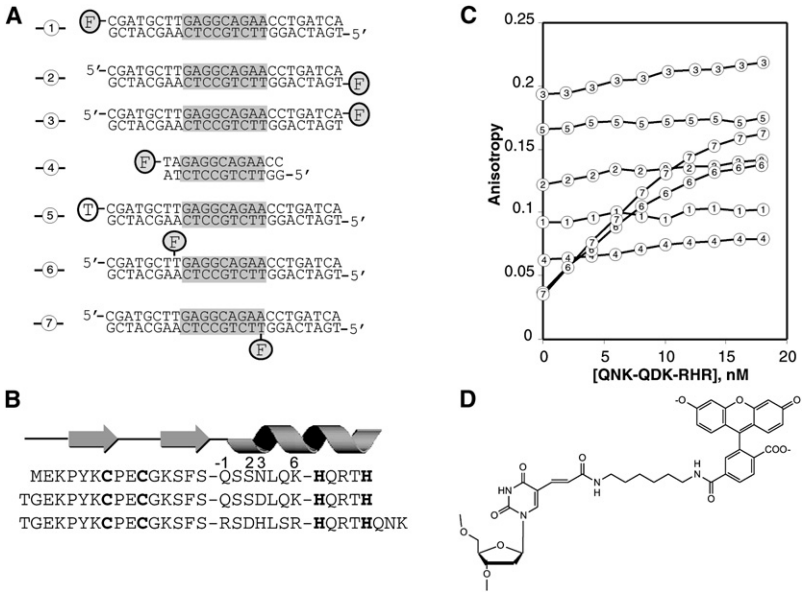

FIGURE 1 (*A*) Sequences of the seven probes evaluated with the QNK-QDK-RHR protein, showing the location of fluorescein [F] or Texas Red [T] labels and the protein-binding site (*boxed*). (*B*) Amino acid sequence of the QNK-QDK-RHR protein, showing metal-binding (*bold*) and DNA-contacting (*numbered*) residues. (*C*) Plots of anisotropy as a function of QNK-QDK-RHR concentration for the seven probes. (*D*) Structure of fluorescein-dT.

probes 6 and 7 showed marked increases in anisotropy in response to protein addition. These two probes have fluorescein labels covalently attached to a modified thymidine base (Fig. 1 *D*) within the probe sequence. In the case of probe 6, the fluorescein-dT is on the more heavily contacted strand, adjacent to the protein-binding site on the 5′ side. Probe 7 has fluorescein-dT on the opposite strand, basepaired to the A at the 3′-end of the binding site. The binding curves obtained with these probes could be fit to dissociation constants of 1.4 ± 0.3 nM (probe 6) and 1.7 ± 0.4 nM (probe 7).

Application to other zinc finger proteins

A second recombinant zinc finger protein was expressed and purified. This protein, which we will refer to as RHR-QDK-QNK, is derived from the first protein, but with the sequences of fingers 1 and 3 interchanged. A schematic structure of this protein is shown in Fig. 2 *B*. As a consequence, this second protein was anticipated to recognize the sequence 5′-GAA-GCA-GAG-3′. A new probe, probe 8, was synthesized to be analogous to probe 7 except that the bases in the protein-binding site were modified to reflect the anticipated binding site for RHR-QDK-QNK. Thus, probe 8 was prepared from the oligonucleotides 5′-CGATGCTTGCAGCAGAGGA TGATCA-3′ and 5′-TGATCA[FdT]CCTCTGCTGCAAG CATCG-3′ (where the core binding site is underlined). These changes required the relocation of the fluorescein-dT base in probe 8 to a position two bases farther away from the protein-binding site. Nonetheless, this probe underwent an anisotropy

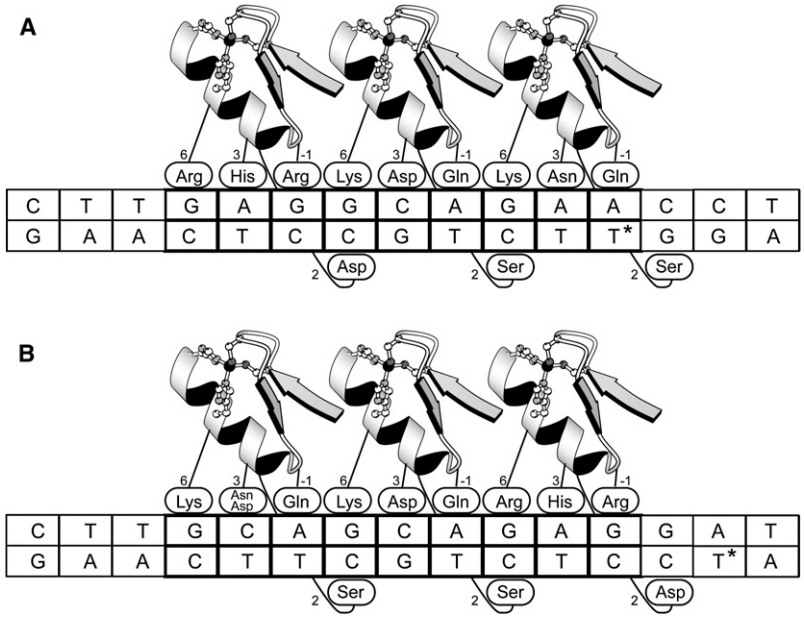

FIGURE 2 Schematic structures for three zinc finger proteins aligned with their binding sites. (*A*) The structure of QNK-QDK-RHR aligned with the binding site used in the probes shown in Fig. 1. The asterisk indicates the position of the fluorescein-dT residue in probe 7. (*B*) The structures of RHR-QDK-Q(N,D)K aligned with the binding site used in probe 8. The asterisk indicates the position of the fluorescein-dT residue in this probe.

change comparable to that of probe 7 in response to protein binding (Fig. 3).

As noted above, QNK-QDK-RHR bound probe 7 with a dissociation constant of 1.7 ± 0.4 nM. This protein bound probe 8 with a much lower affinity (K_d = 730 ± 80 nM). In contrast, RHR-QDK-QNK bound probe 8 with a dissociation constant of 16 ± 3 nM, and had a much lower affinity for probe 7 (K_d = 900 ± 130 nM). Thus, the two proteins show the anticipated discrimination between the two binding sites even though they differ in only two positions out of nine.

Determination of binding specificity

A simple adaptation incorporating unlabeled oligonucleotide competitors provides a rapid assay for the quantitation of binding specificity. Protein is first added to a solution of labeled probe to near saturation, and then this solution is titrated with unlabeled oligonuclotides. The results of such experiments are shown in Fig. 4 *A*. Here, QNK-QDK-RHR was added to a solution of labeled probe 7 until the probe was ~70% bound. This solution was then split between 12 fluorescence cuvettes and a different unlabeled, double-stranded oligonucleotide was titrated into each cuvette. The unlabeled competitors disrupted the protein-probe complex, and the resulting decreases in anisotropy could be fit to yield dissociation constants for each of the protein-unlabeled DNA complexes. In this experiment, each of the 12 competitor oligonucleotides used differed from the probe 7 sequence by a single base change in the 5′-most triplet of the protein-binding site. This triplet is that contacted by the third (C-terminal) zinc finger domain. By systematically varying each position in the triplet to each of the four DNA bases, we were able to determine how tolerant finger 3 is to deviation from its preferred binding site. Consistent with previous work, QNK-QDK-RHR showed a strong preference for 5′-$G^A/_G$G as the 5′-most triplet in its binding site (Fig. 4 *B*). Previous structural studies on this protein (43) revealed that arginine residues in positions −1 and 6 of the recognition helix make bidentate contacts with the guanine bases in the first and last positions of the triplet. The middle position of the triplet is contacted by the residue in position 3 of the recognition helix. In this case, a histidine residue in position 3 makes contact with the N7 of a purine base to confer specificity for A or G.

For comparison, the specificity conferred by finger 3 of the RHR-QDK-QNK protein was determined in the same manner (Fig. 4 *C*). In this case, probe 8 was used as the fluorescent species and all of the competitor oligonucleotides were modified to reflect the preferred binding sequence for this protein. Finger 3 of this second protein was found to specify 5′-$^G/_T$AA, also consistent with previous results for this zinc finger domain in a different position within a protein (43). In this case, the 5′-most position of the triplet is contacted by the lysine residue in position 6, whereas the side-chain carboxamides of Gln in position −1 and Asn in position 3 both make bidentate contacts with adenine bases in the latter two positions of the triplet.

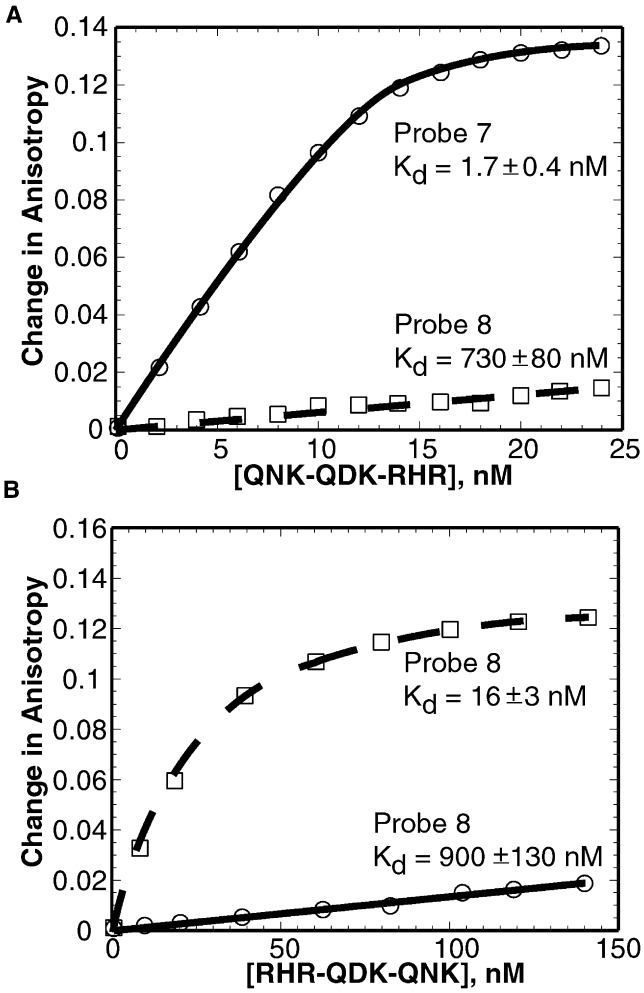

FIGURE 3 Binding curves for two different proteins. Plots of anisotropy as a function of either (*A*) QNK-QDK-RHR or (*B*) RHR-QDK-QNK protein concentration using probe 7 or probe 8 as the labeled DNA. Curves were fit to generate dissociation constants for all four complexes. Not all points are shown for the two lower-affinity complexes. The dissociation constants shown are the mean of three measurements and the uncertainty shown in the standard deviation from the mean derived from these measurements.

High-affinity binding versus high-specificity binding

We next employed our anisotropy-based assay to investigate the correlation between DNA-binding affinity and DNA-binding specificity. To that end, a single amino acid substitution was made to the third finger of the RHR-QDK-Q**N**K protein to produce RHR-QDK-Q**D**K. A schematic structure for this protein is shown in Fig. 2 *B*. It was anticipated that the substitution of Asn in position 3 of the C-terminal finger of RHR-QDK-Q**N**K with Asp would change the binding specificity of the third finger from 5′-$^G/_T$**A**A to 5′-$^G/_T$**C**A (or 5′-$^G/_T$**C** $^A/_G$ (43)). This proved to be the case when the

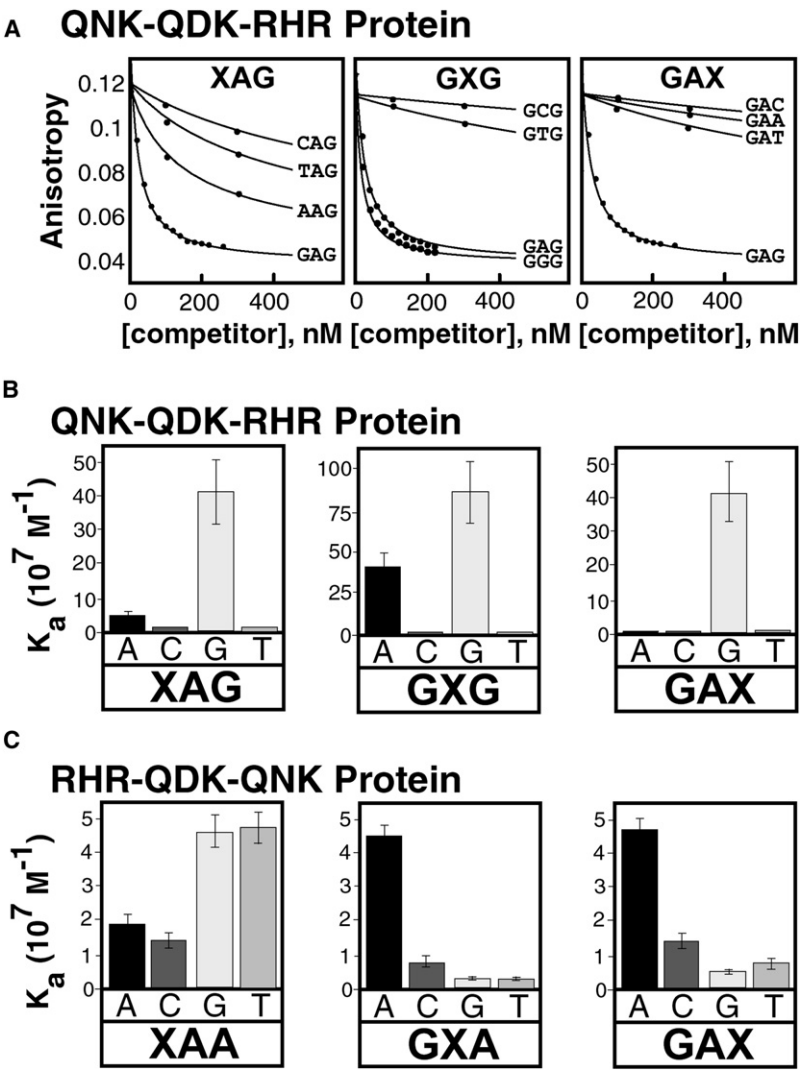

FIGURE 4 Competition experiments to determine binding specificity. (*A*) Plots of anisotropy as a function of competitor DNA concentration for 12 variants of the 5′-most triplet in the QNK-QDK-RHR binding site. First, 15 nM of QNK-QDK-RHR protein were added to a probe 7 solution to bind the majority of the probe. Unlabeled DNA was then added to compete the protein off of the probe, resulting in a decrease in fluorescence anisotropy. Each of the three charts shows plots corresponding to all four bases substituted in the first, second, or third position in the triplet (not all points are shown for lower-affinity complexes). (*B*) The curves in *A* were fit to generate K_a values for each of the 12-point variants in the QNK-QDK-RHR binding site. The resulting binding-site "signature" is a quantitative determination of the preferred base at each position in the triplet. (*C*) The same analysis as in *B* for the RHR-QDK-QNK protein. In this case, probe 8 is the fluorescent species being followed, and each of the 12 oligonucleotide sets used as a competitor is a point variant in the 5′-most triplet of the RHR-QDK-QNK binding site.

binding specificities of the two proteins were evaluated at a reduced salt concentration (50 mM NaCl; Fig. 5, *A* and *B*). Under these conditions, the RHR-QDK-Q**N**K protein bound the 5′-GAA site with a K_d of 1.0 ± 0.6 nM. RHR-QDK-Q**D**K was found to bind its preferred DNA site containing 5′-GCA with fivefold lower affinity (K_d = 5.3 ± 1.3 nM). A direct comparison of the affinities of the two proteins for the four middle position variants reveals significant differences in the extent to which they discriminate between binding sites (Fig. 4 *C*). The RHR-QDK-Q**N**K protein exhibits only a 2.4-fold preference for A over C, the second most highly favored base in the middle position. In contrast, the RHR-QDK-Q**D**K protein displays a ~10-fold preference for C over A. Of interest, the RHR-QDK-Q**N**K protein binds with greater affinity to the 5′-G**C**A-containing target than does the RHR-QDK-Q**D**K protein, even though this is not its preferred binding sequence. Thus, under low-salt concentrations, RHR-QDK-Q**N**K is the higher-affinity protein, but RHR-QDK-Q**D**K exhibits a greater degree of specificity for the same DNA sequence.

These differences in affinity and specificity can be explained on the basis of crystallographically observed contacts (43). In the case of the -Q**N**K domain, the carboxamide side chain of the asparagine in position 3 makes a pair of hydrogen bonds with an adenine base. Because asparagine can act as both a hydrogen-bond donor and acceptor, however, it is also able to interact favorably with donor-acceptor functional groups on the other three bases. As a consequence, this residue shows a relatively modest preference for A. In contrast, the aspartate residue in position 3 of the third finger of RHR-QDK-Q**D**K can only act as a hydrogen-bond acceptor. As such, it could only form hydrogen bonds with the major groove amines of cytosine or adenine. Additionally, the negative charge on this residue likely interacts unfavorably with the electronegative groups present on all of the bases except cytosine. As a result, this amino acid exhibits a high degree of discrimination for cytosine over the other three bases. The reduced binding affinity of this protein is likely also a consequence of the negative charge on Asp-3, as this residue would be expected to

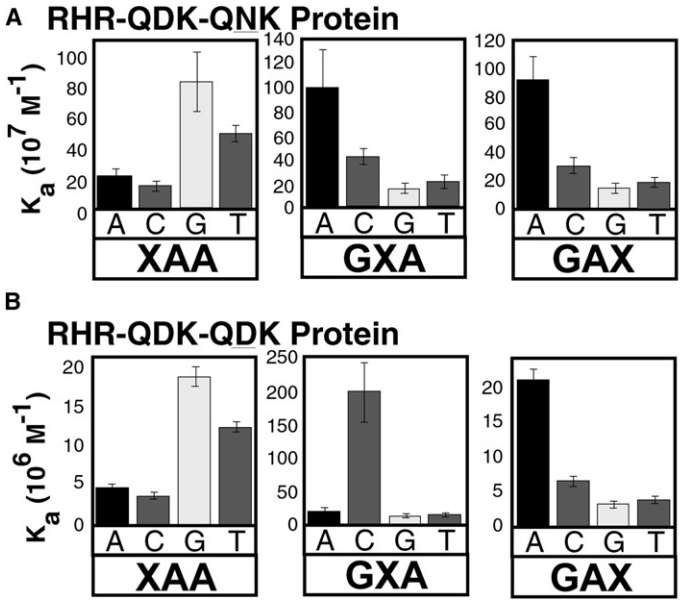

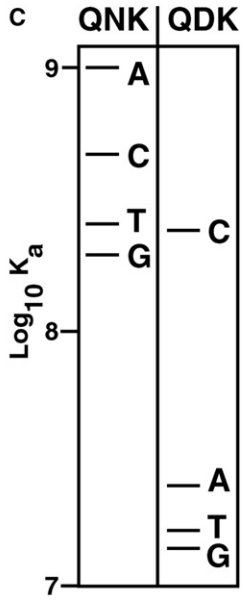

FIGURE 5 (*A*) Association constants for RHR-QDK-Q**N**K binding to probes derived from the sequence -**GAA**-GCA-GAG- in 50 mM NaCl. The ability of this protein to discriminate between bases at each of the three positions within the first base triplet is shown. (*B*) Corresponding association constants for RHR-QDK-QDK. (*C*) Summary of the derived association constants for probes with the sequence -G**X**A-GCA-GAG- for the proteins RHR-QDK-Q**N**K and RHR-QDK-Q**D**K.

interact unfavorably with the negatively charged DNA backbone.

Effects of NaCl concentration on DNA-binding specificity

We also investigated the role that electrostatic interactions play in conferring the two binding specificities of the proteins. For a number of protein-DNA complexes, the association constant shows a strong dependence on salt concentration (44–52). Because the initial binding-site determination experiments were conducted under relatively low salt conditions (50 mM NaCl), we repeated the binding assays for both proteins at gradually increasing concentrations of salt up to 100 mM NaCl. We determined equilibrium constants for the two proteins bound to all four of the DNA targets varying in the middle position of the triplet. The two proteins demonstrated significantly different responses to changing salt concentration, as shown in Fig. 6. For all protein-DNA complexes examined, the double-logarithmic plot of K_a as a function of [NaCl] is linear, consistent with previous reports for different DNA-binding proteins. Strikingly, all four plots obtained with the RHR-QDK-Q**N**K protein have comparable slopes ($m_{avg} = -4.7 \pm 0.5$), indicating that the binding preference of this protein at the middle position of the triplet is insensitive to ionic strength. Thus, increasing salt decreases the protein's affinity for DNA in general, but has no effect on its ability to discriminate between bases at this position. In contrast, the four plots obtained with the RHR-QDK-Q**D**K protein show significant differences in sensitivity to NaCl concentration. Plots for three sites (with A, G, and T) show comparable slopes with an average of -3.4 ± 0.3. However, the plot for the preferred site (with C) exhibits heightened salt sensitivity with a slope of -6.5 ± 0.2. These data indicate that this protein loses its ability to recognize C as the NaCl concentration is increased, suggesting a significant role for the negative charge on Asp-3 in mediating base contacts. Thus, RHR-QDK-QDK exhibits changes in both affinity and specificity in response to changes in salt concentration.

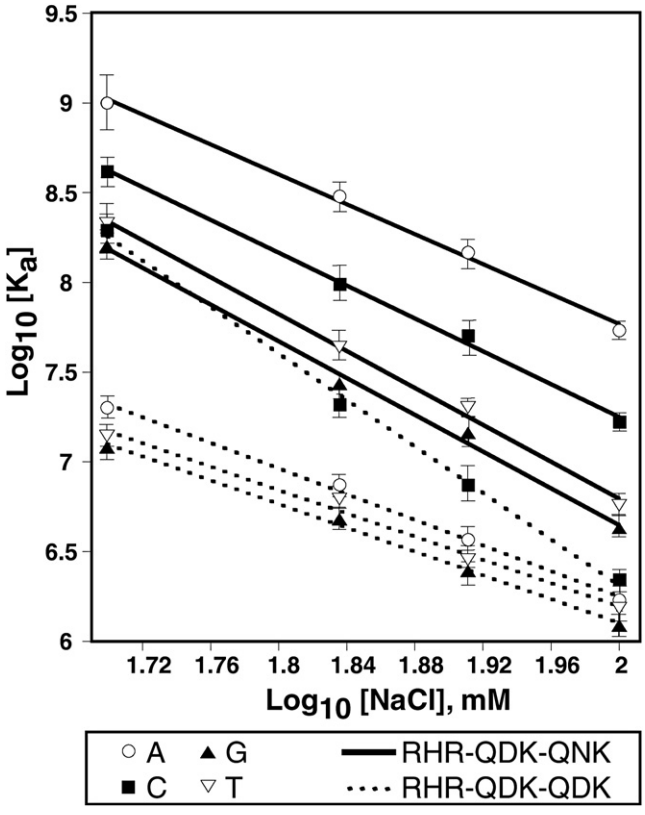

FIGURE 6 NaCl-concentration dependence of the binding affinity of the RHR-QDK-Q**N**K and RHR-QDK-Q**D**K proteins for probes including the sequence -G**X**A-GCA-GAG-. The logarithm of the K_a for each interaction is plotted as a function of the logarithm of the NaCl concentration.

Numerous previous publications have reported that DNA-binding specificity typically improves with increasing salt concentration. This apparent discrepancy is due to differences in experimental setups. In general, protein-DNA interactions can be divided into a nonspecific component mediated primarily by contacts to the DNA backbone, and a sequence-specific component mediated primarily by contacts to individual bases. The first component is dominated by electrostatic interactions between basic residues in the protein and phosphate groups in the DNA backbone. These electrostatic interactions are expected to decrease in strength with increasing salt concentration. Sequence-specific contacts typically involve hydrogen bonds or van der Waals interactions between amino acid side chains and specific combinations of functional groups on the DNA bases. In general, these interactions are expected to be substantially less sensitive to salt concentration. Most previous publications concerning the effects of ionic strength on DNA-binding specificity compared only random (completely nonspecific) and optimal (completely specific) DNA sites. Because nonspecific complexes are dominated by electrostatic interactions, DNA-binding specificity is seen to improve with increasing salt concentration when only random (completely nonspecific) and optimal binding sites are compared. In this work, all binding sites are specific and differ by only one base out of nine from preferred binding sites.

Our results indicate that a specific base contact can also be sensitive to salt concentration. The interaction between Asp-3 in the third finger of the RHR-QDK-Q**D**K and its preferred cytosine base shows an unusually strong dependence on ionic strength, suggesting that the negative charge on this amino acid mediates a favorable interaction with this particular DNA base. This additional electrostatic interaction is weakened as the NaCl concentration is increased, leading to a more rapid decrease in affinity for the cytosine-containing DNA site than is observed for this protein in complex with any of the other three sites. Thus, DNA-binding specificity at this position is reduced with increasing ionic strength.

DISCUSSION

In this work, a fluorescence-based assay was used to examine the binding affinities and specificities of Cys_2His_2 zinc finger proteins. Although this assay has many advantages, it does require the preparation of appropriately labeled DNA probes and does not allow direct observation of both bound and unbound species. This assay enabled us to observe subtle features in DNA recognition by zinc finger proteins and quantitatively evaluate binding specificity at the level of individual base contacts. By performing a direct comparison of two zinc finger mutants, we were able to demonstrate that a protein with the highest affinity for a given site need not be the protein with the highest level of discrimination for all sequence features within that site. This finding has significant implications for the construction of zinc finger domains by phage display and other experimental selection techniques, as these approaches typically select for proteins that recognize their DNA target with the highest possible affinity rather than those that discriminate well between the intended target site and other, related DNA sites. In addition, our finding that the ability of a protein to discriminate between bases can be impaired by increasing ionic strength highlights the importance of conducting in vitro selection and characterization experiments under conditions similar to the intracellular environment in which those proteins are expected to function. We observed a very significant loss in binding specificity in the RHR-QDK-QDK protein over a fairly narrow range of salt concentrations. By 100 mM NaCl, the protein had lost all ability to discriminate between bases at the middle position of the first triplet. This value is well below the 140 mM typically assumed to represent intracellular ionic strength.

CONCLUSIONS

It is possible to design zinc finger proteins that recognize particular DNA sequences with considerable specificity and affinity. In an appropriate context, the presence of asparagine in position 3 results in specificity for A in the central position of a zinc finger recognition site. Analogously, the presence of aspartate in the same position results in specificity for C. A comparison of the detailed binding properties demonstrates that the protein with asparagine actually has a higher affinity for the target oligonucleotide with C in the central position than does the protein with aspartate. Thus, in this context, the protein with the highest affinity for a given target is not necessarily the one that shows the highest preference for this target. Aspartate with its negative charge is unusual in that most of the residues that participate most effectively in contacts with DNA are either neutral or positively charged. The impact of this negatively residue is reflected in the relatively steep dependence of the binding affinity of the protein that bears this residue on NaCl concentration. The studies presented here were facilitated by the use of fluorescence anisotropy-based binding assays that allowed precise determination of binding affinities under a wide range of solution conditions.

We thank Drs. Anthony Guerrerio, Gregory J. Gatto Jr., and Barbara Amann for advice and assistance.

This work was supported by the Intramural Research Program of the National Institute of Diabetes and Digestive and Kidney Diseases, and by the National Institute of General Medical Sciences.

REFERENCES

1. Beerli, R. R., and C. F. Barbas, 3rd. 2002. Engineering polydactyl zinc-finger transcription factors. *Nat. Biotechnol.* 20:135–141.
2. Jantz, D., B. T. Amann, …, J. M. Berg. 2004. The design of functional DNA-binding proteins based on zinc finger domains. *Chem. Rev.* 104:789–799.

3. Klug, A. 1999. Zinc finger peptides for the regulation of gene expression. *J. Mol. Biol.* 293:215–218.
4. Pabo, C. O., E. Peisach, and R. A. Grant. 2001. Design and selection of novel Cys_2His_2 zinc finger proteins. *Annu. Rev. Biochem.* 70:313–340.
5. Segal, D. J., B. Dreier, …, C. F. Barbas, 3rd. 1999. Toward controlling gene expression at will: selection and design of zinc finger domains recognizing each of the 5′-GNN-3′ DNA target sequences. *Proc. Natl. Acad. Sci. USA.* 96:2758–2763.
6. Liu, P. Q., E. J. Rebar, …, A. P. Wolffe. 2001. Regulation of an endogenous locus using a panel of designed zinc finger proteins targeted to accessible chromatin regions. Activation of vascular endothelial growth factor A. *J. Biol. Chem.* 276:11323–11334.
7. Ordiz, M. I., C. F. Barbas, 3rd, and R. N. Beachy. 2002. Regulation of transgene expression in plants with polydactyl zinc finger transcription factors. *Proc. Natl. Acad. Sci. USA.* 99:13290–13295.
8. Rebar, E. J., Y. Huang, …, F. J. Giordano. 2002. Induction of angiogenesis in a mouse model using engineered transcription factors. *Nat. Med.* 8:1427–1432.
9. Beumer, K. J., J. K. Trautman, …, D. Carroll. 2008. Efficient gene targeting in *Drosophila* by direct embryo injection with zinc-finger nucleases. *Proc. Natl. Acad. Sci. USA.* 105:19821–19826.
10. Bibikova, M., D. Carroll, …, S. Chandrasegaran. 2001. Stimulation of homologous recombination through targeted cleavage by chimeric nucleases. *Mol. Cell. Biol.* 21:289–297.
11. Carroll, D., K. J. Beumer, …, J. K. Trautman. 2008. Gene targeting in *Drosophila* and *Caenorhabditis elegans* with zinc-finger nucleases. *Methods Mol. Biol.* 435:63–77.
12. Carroll, D., J. J. Morton, …, D. J. Segal. 2006. Design, construction and in vitro testing of zinc finger nucleases. *Nat. Protoc.* 1:1329–1341.
13. Doyon, Y., J. M. McCammon, …, S. L. Amacher. 2008. Heritable targeted gene disruption in zebrafish using designed zinc-finger nucleases. *Nat. Biotechnol.* 26:702–708.
14. Maeder, M. L., S. Thibodeau-Beganny, …, J. K. Joung. 2008. Rapid ''open-source'' engineering of customized zinc-finger nucleases for highly efficient gene modification. *Mol. Cell.* 31:294–301.
15. Porteus, M. H., and D. Baltimore. 2003. Chimeric nucleases stimulate gene targeting in human cells. *Science.* 300:763.
16. Remy, S., L. Tesson, …, I. Anegon. 2009. Zinc-finger nucleases: a powerful tool for genetic engineering of animals. *Transgenic Res.,* Sep 26 [Epub ahead of print].
17. Shukla, V. K., Y. Doyon, …, F. D. Urnov. 2009. Precise genome modification in the crop species Zea mays using zinc-finger nucleases. *Nature.* 459:437–441.
18. Townsend, J. A., D. A. Wright, …, D. F. Voytas. 2009. High-frequency modification of plant genes using engineered zinc-finger nucleases. *Nature.* 459:442–445.
19. Berg, J. M. 1988. Proposed structure for the zinc-binding domains from transcription factor IIIA and related proteins. *Proc. Natl. Acad. Sci. USA.* 85:99–102.
20. Lee, M. S., G. P. Gippert, …, P. E. Wright. 1989. Three-dimensional solution structure of a single zinc finger DNA-binding domain. *Science.* 245:635–637.
21. Pavletich, N. P., and C. O. Pabo. 1991. Zinc finger-DNA recognition: crystal structure of a Zif268-DNA complex at 2.1 A. *Science.* 252:809–817.
22. Beerli, R. R., D. J. Segal, …, C. F. Barbas, 3rd. 1998. Toward controlling gene expression at will: specific regulation of the erbB-2/HER-2 promoter by using polydactyl zinc finger proteins constructed from modular building blocks. *Proc. Natl. Acad. Sci. USA.* 95:14628–14633.
23. Desjarlais, J. R., and J. M. Berg. 1992. Toward rules relating zinc finger protein sequences and DNA binding site preferences. *Proc. Natl. Acad. Sci. USA.* 89:7345–7349.
24. Desjarlais, J. R., and J. M. Berg. 1993. Use of a zinc-finger consensus sequence framework and specificity rules to design specific DNA binding proteins. *Proc. Natl. Acad. Sci. USA.* 90:2256–2260.
25. Desjarlais, J. R., and J. M. Berg. 1994. Length-encoded multiplex binding site determination: application to zinc finger proteins. *Proc. Natl. Acad. Sci. USA.* 91:11099–11103.
26. Greisman, H. A., and C. O. Pabo. 1997. A general strategy for selecting high-affinity zinc finger proteins for diverse DNA target sites. *Science.* 275:657–661.
27. Khopde, S., E. E. Biswas, and S. B. Biswas. 2002. Affinity and sequence specificity of DNA binding and site selection for primer synthesis by *Escherichia coli* primase. *Biochemistry.* 41:14820–14830.
28. Negi, S., M. Imanishi, …, Y. Sugiura. 2008. New redesigned zinc-finger proteins: design strategy and its application. *Chemistry (Easton).* 14:3236–3249.
29. Rebar, E. J., H. A. Greisman, and C. O. Pabo. 1996. Phage display methods for selecting zinc finger proteins with novel DNA-binding specificities. *Methods Enzymol.* 267:129–149.
30. Rebar, E. J., and C. O. Pabo. 1994. Zinc finger phage: affinity selection of fingers with new DNA-binding specificities. *Science.* 263:671–673.
31. Sander, J. D., P. Zaback, …, D. Dobbs. 2007. Zinc Finger Targeter (ZiFiT): an engineered zinc finger/target site design tool. *Nucleic Acids Res.* 35:W599–W605.
32. Sander, J. D., P. Zaback, …, D. Dobbs. 2009. An affinity-based scoring scheme for predicting DNA-binding activities of modularly assembled zinc-finger proteins. *Nucleic Acids Res.* 37:506–515.
33. Segal, D. J., J. W. Crotty, …, N. C. Horton. 2006. Structure of Aart, a designed six-finger zinc finger peptide, bound to DNA. *J. Mol. Biol.* 363:405–421.
34. Wolfe, S. A., R. A. Grant, and C. O. Pabo. 2003. Structure of a designed dimeric zinc finger protein bound to DNA. *Biochemistry.* 42:13401–13409.
35. Wolfe, S. A., H. A. Greisman, …, C. O. Pabo. 1999. Analysis of zinc fingers optimized via phage display: evaluating the utility of a recognition code. *J. Mol. Biol.* 285:1917–1934.
36. Wolfe, S. A., L. Nekludova, and C. O. Pabo. 2000. DNA recognition by Cys_2His_2 zinc finger proteins. *Annu. Rev. Biophys. Biomol. Struct.* 29:183–212.
37. Wolfe, S. A., E. I. Ramm, and C. O. Pabo. 2000. Combining structure-based design with phage display to create new $Cys_{(2)}His_{(2)}$ zinc finger dimers. *Structure.* 8:739–750.
38. Heyduk, T., and J. C. Lee. 1990. Application of fluorescence energy transfer and polarization to monitor *Escherichia coli* cAMP receptor protein and lac promoter interaction. *Proc. Natl. Acad. Sci. USA.* 87:1744–1748.
39. Heyduk, T., Y. Ma, …, R. H. Ebright. 1996. Fluorescence anisotropy: rapid, quantitative assay for protein-DNA and protein-protein interaction. *Methods Enzymol.* 274:492–503.
40. LeTilly, V., and C. A. Royer. 1993. Fluorescence anisotropy assays implicate protein-protein interactions in regulating trp repressor DNA binding. *Biochemistry.* 32:7753–7758.
41. Jantz, D., and J. M. Berg. 2004. Reduction in DNA-binding affinity of Cys_2His_2 zinc finger proteins by linker phosphorylation. *Proc. Natl. Acad. Sci. USA.* 101:7589–7593.
42. Wang, Z. X. 1995. An exact mathematical expression for describing competitive binding of two different ligands to a protein molecule. *FEBS Lett.* 360:111–114.
43. Kim, C. A., and J. M. Berg. 1996. A 2.2 A resolution crystal structure of a designed zinc finger protein bound to DNA. *Nat. Struct. Biol.* 3:940–945.
44. Baud, S., E. Margeat, …, N. Poujol. 2002. Equilibrium binding assays reveal the elevated stoichiometry and salt dependence of the interaction between full-length human sex-determining region on the Y chromosome (SRY) and DNA. *J. Biol. Chem.* 277:18404–18410.
45. Boyer, M., N. Poujol, …, C. A. Royer. 2000. Quantitative characterization of the interaction between purified human estrogen receptor α and DNA using fluorescence anisotropy. *Nucleic Acids Res.* 28:2494–2502.
46. Frank, D. E., R. M. Saecker, …, M. T. Record, Jr. 1997. Thermodynamics of the interactions of lac repressor with variants of the symmetric

lac operator: effects of converting a consensus site to a non-specific site. *J. Mol. Biol.* 267:1186–1206.

47. Hart, D. J., R. E. Speight, …, J. M. Blackburn. 1999. The salt dependence of DNA recognition by NF-κB p50: a detailed kinetic analysis of the effects on affinity and specificity. *Nucleic Acids Res.* 27:1063–1069.
48. Lohman, T. M., C. G. Wensley, …, M. T. Record, Jr. 1980. Use of difference boundary sedimentation velocity to investigate nonspecific protein-nucleic acid interactions. *Biochemistry.* 19:3516–3522.
49. Ozers, M. S., J. J. Hill, …, J. Gorski. 1997. Equilibrium binding of estrogen receptor with DNA using fluorescence anisotropy. *J. Biol. Chem.* 272:30405–30411.
50. Record, Jr., M. T., P. L. deHaseth, and T. M. Lohman. 1977. Interpretation of monovalent and divalent cation effects on the lac repressor-operator interaction. *Biochemistry.* 16:4791–4796.
51. Record, Jr., M. T., J. H. Ha, and M. A. Fisher. 1991. Analysis of equilibrium and kinetic measurements to determine thermodynamic origins of stability and specificity and mechanism of formation of site-specific complexes between proteins and helical DNA. *Methods Enzymol.* 208:291–343.
52. Speight, R. E., D. J. Hart, and J. M. Blackburn. 2002. Distamycin A affects the stability of NF-κB p50-DNA complexes in a sequence-dependent manner. *J. Mol. Recognit.* 15:19–26.